Research Article

Cancer Immunology Research

Endogenous CD4$^+$ T Cells Recognize Neoantigens in Lung Cancer Patients, Including Recurrent Oncogenic *KRAS* and *ERBB2* (*Her2*) Driver Mutations

Joshua R. Veatch[1], Brenda L. Jesernig[1], Julia Kargl[1,2], Matthew Fitzgibbon[1], Sylvia M. Lee[3], Christina Baik[3], Renato Martins[3], A. McGarry Houghton[1], and Stanley R. Riddell[1]

Abstract

T cells specific for neoantigens encoded by mutated genes in cancers are increasingly recognized as mediators of tumor destruction after immune-checkpoint inhibitor therapy or adoptive cell transfer. Much of the focus has been on identifying epitopes presented to CD8$^+$ T cells by class I MHC. However, CD4$^+$ class II MHC-restricted T cells have been shown to have an important role in antitumor immunity. Unfortunately, the vast majority of neoantigens recognized by CD8$^+$ or CD4$^+$ T cells in cancer patients result from random mutations and are patient-specific. Here, we screened the blood of 5 non–small cell lung cancer (NSCLC) patients for T-cell responses to candidate mutation-encoded neoepitopes. T-cell responses were detected to 8.8% of screened antigens, with 1 to 7 antigens identified per patient. A majority of responses were to random, patient-specific mutations. However, CD4$^+$ T cells that recognized the recurrent *KRAS*^{G12V} and the *ERBB2* (*Her2*) internal tandem duplication (ITD) oncogenic driver mutations, but not the corresponding wild-type sequences, were identified in two patients. Two different T-cell receptors (TCR) specific for *KRAS*^{G12V} and one T-cell receptor specific for *Her2*-ITD were isolated and conferred antigen specificity when transfected into T cells. Deep sequencing identified the *Her2*-ITD–specific TCR in the tumor but not nonadjacent lung. Our results showed that CD4$^+$ T-cell responses to neoantigens, including recurrent driver mutations, can be derived from the blood of NSCLC patients. These data support the use of adoptive transfer or vaccination to augment CD4$^+$ neoantigen-specific T cells and elucidate their role in human antitumor immunity.

Introduction

T cells can eliminate cancer cells through recognition of peptides derived from the processing of nonmutated or mutated proteins and presented bound to cell-surface MHC molecules. T cells specific for neoantigens encoded by mutated genes have been implicated as important mediators of antitumor immunity in patients receiving checkpoint blocking antibodies (1) and adoptive T-cell transfer (2, 3). Neoantigens are attractive targets for T cells because they are not subject to central and peripheral tolerance mechanisms that limit the frequency and function of T cells specific for self-antigens (4). Indeed, the burden of somatic mutations present in non–small cell lung cancer (NSCLC) and other cancers correlates with response to immune-checkpoint inhibitors (5, 6), suggesting that reinvigoration of endogenous neoantigen-reactive T cells contributes to efficacy. Clinical response in patients with melanoma and cervical cancer treated with tumor-infiltrating lymphocytes (TIL) has also correlated with the presence of neoantigen-reactive T cells in the TIL product (2, 3). Most neoantigens are derived from random, patient-specific mutations that may be heterogeneously expressed in tumors, which limits their utility as targets for adoptive transfer across multiple patients (4), and can allow escape of antigen-negative tumor cells (7). Recurrent oncogenic driver mutations are expressed homogenously in cancers from many patients and, if immunogenic, would represent ideal targets for immunotherapy.

Several oncogenic mutations have been described in NSCLC. Mutations of *KRAS* that lead to constitutive growth signaling are present in 20% of NSCLC and 40% of colorectal cancers, with the recurrent G12V mutation making up 20% to 40% of activating *KRAS* mutations across tumor types (8). A four-amino acid in-frame insertion in exon 20 of Her2 leads to constitutive growth signaling in 2% to 4% of NSCLC (9). Unfortunately, unlike other driver mutations, such as *ALK*, *ROS1*, and *EGFR* in lung cancer, effective inhibitors of *KRAS* and *Her2* oncoproteins are not available for patients (10). Efforts to identify T-cell responses arising from oncogenic mutations have largely focused on class I MHC to CD8$^+$ T cells and are rarely successful, perhaps as a consequence of immune selection based on HLA genotype (11, 12), or the development of irreversible T-cell exhaustion that precludes detecting reactive T cells using functional assays (13). A role for CD4$^+$ class II MHC-restricted T cells in human antitumor

[1]Immunotherapy Integrated Research Center, Clinical Research Division, Fred Hutchinson Cancer Research Center, Seattle, Washington. [2]Otto Loewi Research Center, Pharmacology, Medical University of Graz, Graz, Austria. [3]Division of Medical Oncology, University of Washington, Seattle, Washington.

Note: Supplementary data for this article are available at Cancer Immunology Research Online (http://cancerimmunolres.aacrjournals.org/).

Corresponding Author: Joshua R. Veatch, Fred Hutchinson Cancer Research Center, 1100 Fairview Avenue North, 505 N 72nd St., Seattle, WA 98109. Phone: 206-667-5108; Fax: 206-667-5894; E-mail: jveatch@fhcrc.org

Cancer Immunol Res 2019;7:910–22

doi: 10.1158/2326-6066.CIR-18-0402

immunity is increasingly being appreciated, despite the absence of class II MHC on many tumors. $CD4^+$ T cells can recognize tumor antigen presented by professional antigen-presenting cells (APC) and support the priming and expansion of $CD8^+$ T cells in lymphoid tissues, and the effector function of T cells and innate immune cells in the tumor microenvironment. Recent work in mouse models has suggested that $CD4^+$ T cells at the site of the tumor and systemically are a critical component of immune-mediated tumor rejection (14), and that vaccination to augment class II MHC-restricted $CD4^+$ T cells to neoantigens can have potent therapeutic effects (15). $CD4^+$ T-cell responses to neoantigens are common in patients with melanoma (16), and a study in melanoma patients vaccinated with candidate neoantigen peptides intending to induce $CD8^+$ T-cell responses instead led to $CD4^+$ T-cell responses to 60% of the peptides, with evidence of antitumor activity (17). Peritumoral $CD4^+$ T cells have also been associated with an improved prognosis in NSCLC (18–20). Here, we report that neoantigen-specific $CD4^+$ T-cell responses can be detected in patients with NSCLC, and we identified driver mutations in $KRAS^{G12V}$ and *Her2*-ITD as targets for $CD4^+$ T cells. The isolation of T-cell receptors (TCR) specific for these mutations makes it feasible to evaluate adoptive transfer of TCR-engineered T cells to augment immunity in cancers with the appropriate MHC type driven by these mutations.

Materials and Methods

Clinical protocol

This study was performed at the Fred Hutchinson Cancer Research Center (FHCRC) using NSCLC tissue and nonadjacent lung tissue (as far removed from the malignant lesion as possible, at least 3 cm) obtained after informed consent from 4 patients (1347, 1490, 1238, and 1139) enrolled on a protocol, including patients undergoing curative intent resections for stage I–III NSCLC approved by the institutional review board (IRB). Formalin-fixed, paraffin-embedded tissue from a lymph node resection was obtained from one patient (511), and peripheral blood samples were obtained from patients 511, 1139, and 1238 on a protocol enrolling adult patients with a cancer diagnosis who were willing to donate blood and tumor samples. Leukapheresis products were obtained from patients 1347 and 1490 on a protocol enrolling adult patients with a cancer diagnosis approved by the IRB. All studies excluded patients with a medical contraindication to blood donation or leukapheresis, and were conducted in accordance with the Belmont Report.

Patient information

Patient 511 was a 73-year-old woman former smoker who presented at the age of 70 with lung adenocarcinoma metastatic to lymph nodes and bone. She was treated with carboplatin and pemetrexed followed by pemetrexed monotherapy, and was in a period of long-term disease stability 3 years after diagnosis when blood donation occurred.

Patient 1347 was a 64-year-old male former smoker who presented with a stage IIB squamous cell carcinoma treated with surgical resection followed by adjuvant carboplatin and paclitaxel. At the time of blood donation, he was in surveillance with no evidence of disease.

Patient 1490 was a 62-year-old female former smoker who initially presented with pT2a lung adenocarcinoma that was resected, but subsequently had perihilar and mediastinal local recurrence. She donated blood following the initiation of definitive chemoradiation treatment with carboplatin and paclitaxel.

Patient 1139 was a 69-year-old female former smoker who initially had resection of a stage I lung adenocarcinoma and subsequently had local recurrence and brain metastasis treated with stereotactic radiosurgery followed by carboplatin and pemetrexed for 4 cycles followed by pemetrexed maintenance for 6 cycles. Disease progression occurred, and she was treated with nivolumab, and this was followed by disease progression. The patient donated blood while being treated with nivolumab.

Patient 1238 was a 68-year-old nonsmoking man who initially presented with stage IIIA lung adenocarcinoma treated with resection followed by adjuvant pemetrexed and cisplatin, which was followed by progression to metastatic disease 1 year later. The patient was treated with afatanib followed by progression and pembrolizumab followed by progression. The patient then had docetaxel and ramicirumab followed by ramicirumab maintenance, which he was on at the time of his blood donation.

Selection of mutations for screening

For each patient, single-nucleotide variants (SNV) were determined by comparison with normal DNA samples and ranked by variant allele frequency and expression to select candidate peptides for screening. For patient 511, mutations called by MuTect 1.1.7 (21) and Strelka 1.0.14 (22) with variant allele frequency greater than 20% were ranked by mean expression in The Cancer Genome Atlas (TCGA) for lung adenocarcinoma, and the top 45 mutations were screened. For patient 1490, all SNVs identified by both MuTect 1.1.7 and Strelka 1.0.14 had variant allele frequencies of 10% to 40%. These were ranked by mean expression in the TCGA for lung adenocarcinoma, and the top 46 mutations were screened. For patient 1139, SNVs called by both MuTect 1.1.7 and Strelka 1.0.14 with variant allele frequency of greater than 20% were ranked by mean expression in the TCGA for lung adenocarcinoma, and the top 46 mutations were screened. For patient 1238, <50 mutations were detected, so SNVs called by either MuTect 1.1.7 or Strelka 1.0.14 were ranked by mean expression in the TCGA for lung adenocarcinoma, and SNVs with expression greater than 3 transcripts per million (TPM) were screened.

Somatic variant calling for patient 1347 revealed a large number (>10,000) of C>A/G>T transversions, with low variant allele frequency. A similar number of variants with similar properties were found in the corresponding normal sample as well, suggesting that these were artifacts likely due to oxidation during DNA shearing (20). To avoid this issue with this particular sample, we leveraged RNA-seq data from the corresponding patient-derived xenograft (PDX). We first aligned the PDX RNA-seq to the mouse genome (mm9 release of the mouse genome) to suppress reads arising from the mouse. Variant calling on the remaining reads was performed according to the Broad Institute's GATK "Best Practices" RNA-seq variant calling workflow, including two-pass STAR alignment, splitting of spliced reads, and application of the HaplotypeCaller (23) ignoring soft-masked bases (https://software.broadinstitute.org/gatk/documentation/article.php?id=3891). The HaplotypeCaller was also used to call germline variants in the corresponding normal blood exome sample. We retained variants found by RNA-seq and not observed in the germline exome capture. To capture additional candidate variants, we also used the MuTect somatic variant caller to compare the analysis-ready PDX RNA-seq BAM file or the PDX exome-capture BAM file against the normal blood exome BAM file. Missense mutations

identified through all of the above processes were merged into a set of 235 candidate variants that were all manually inspected with the Integrative Genomics Viewer (IGV; ref. 23) to retain those supported by the resected tumor exome and the PDX but not observed in the normal blood exome data. Variants were ranked by number of RNA-seq reads supporting the alternate allele at each position, and the top 57 mutations were selected for peptide synthesis.

Unlike MuTect 1.1.7, the Strelka variant caller reports candidate somatic insertions and deletions. The fewer than 25 indels reported were manually inspected and subjected to similar filtering criteria as the above point mutations, including variant allele frequency and expected expression of containing gene (aggregated from TCGA lung adenocarcinoma or measured directly from 1347 PDX). Frameshifts likely to cause the resulting protein to be subject to nonsense-mediated decay were also excluded. Apart from the *Her2*-ITD found in patient 1238, no protein-coding indels not predicted to be subject to nonsense-mediated decay were identified. The criterion for induction of nonsense mediate decay is the creation of a stop codon before the terminal exon of the transcript.

T-cell culture

Peripheral blood mononuclear cells (PBMC) were isolated from the blood of patients and normal donors using gradient density centrifugation using lymphocyte separation medium (Corning), and washed 3 times with PBS supplemented with EDTA (3.6 mmol/L). Patient PBMCs were stimulated with overlapping 20-mer peptides (synthesized by Elim Biopharma). Two peptides spanning each mutation with the mutated residue at position +7 or +13 of the 20-amino acid sequence were used for stimulation, with pools of up to 100 peptides encompassing 50 mutations used for stimulations. Subsequent experiments to analyze T-cell reactivity were performed with single 27-mer peptides (>80% purity), with the mutant or wild-type amino acid at position +13.

Cryopreserved PBMCs (30–120 million) were thawed and rested overnight in RPMI media with L-glutamine (300 mg/L) and HEPES (25 mmol/L; both Gibco) supplemented with 10% human serum (produced in house from pooled healthy donors who provided informed consent and heat-inactivated), 50 μmol/L beta-mercaptoethanol, penicillin (100 U/mL), streptomycin (100U/mL), an additional 4 mmol/L L-glutamine (termed CTL media), and recombinant human IL7 (2 ng/mL; PeproTech). The following morning, PBMCs were washed, and 10^7 cells were plated in individual wells of a 6-well plate in 5 mL CTL media containing a pool of each peptide (1 μg/mL) without cytokines. Recombinant IL2 (PeproTech) was added to a final concentration of 10 U/mL on day +3, and half-media changes with supplemental IL2 were performed on days +3, +6, and +9. On day +13, cells from individual wells were harvested and assayed by ELISA and/or cytokine staining assays, as described below.

Enrichment of T cells identified to be reactive in the initial assay was performed following a stimulation of PBMCs using one or several (as many as 5 pooled) purified mutant peptides and additional cytokines that improved the efficiency of growth with initial stimulation and in subsequent limiting dilution cultures. Briefly, PBMCs were first stimulated with 27-mer mutant peptides (1 μg/mL) in the presence of IL21 (30 ng/mL), IL7 (5 ng/mL), IL15 (1 ng/mL), and IL2 (10 U/mL; all cytokines from PeproTech) for 13 days, and the cultures were then restimulated with autologous B cells (isolated and stimulated as described below) pulsed with a single 27-mer peptide (20 μg/mL) for 4 hours, followed by staining and sorting live, IFNγ-secreting T cells (Interferon secretion kit APC, Miltenyi; cat. 130-090-762, with included capture and detection reagents), as well as with anti-CD4–pacific blue (clone RPA 14, BioLegend; cat. 300521) and anti CD8–FITC (clone HIT8a, BD Pharmingen; cat. 555634) on a FACS Aria2 (BD Biosciences).

Sorted T cells included antigen-specific cells, as well as cells that nonspecifically produced IFNγ, with unknown purity. In order to isolate clonal or oligoclonal cell populations that were antigen-specific, sorted cells (3 or 10 cells per well) were expanded at limiting dilution in a 96-well plate in the presence of 1.0×10^5 irradiated allogeneic PBMCs, phytohemagglutinin (2 μg/mL; Sigma), and IL2 (100 U/mL) for 14 to 20 days, with additional IL2 supplemented at day 14. After expansion, T cells (10,000–100,000 cells) were incubated with autologous B cells (100,000) pulsed with mutant peptides (10 μg/mL), and IFNγ production was measured by ELISA (as described below) to identify those with antigen specificity. Reactive lines were then expanded using a rapid expansion protocol described previously and cryopreserved (in CTL medium supplemented with 10% DMSO and additional 10% human serum (for a final concentration of 20% human serum; ref. 24). Cryopreserved cells were thawed and rested overnight in CTL media supplemented with IL2 (10 U/mL) prior to assays.

For culture of TILs, we used methods described previously (25). Briefly, 6 to 12 fragments of patient-derived tumor tissue ($2 \times 2 \times 2$ mm) were cultured in 24-well plates in T-cell media (RPMI-1640, 10% fetal calf serum, 10 mmol/L HEPES, 100 U/mL penicillin, 100U/mL streptomycin, 50 μg/mL gentamicin, 50 μmol/L beta-mercaptoethanol) in the presence of IL2 (6,000 U/mL) for 35 days. TILs were passaged when confluent. Following the conclusion of the 35-day expansion protocol, cells were cryopreserved prior to use in immunologic assays.

Cell lines

HLA-typed B lymphoblastoid cell lines (B-LCL) BM14, DEM, LUY, CB6B, and DEU were obtained from the research cell bank. The remainder of the B-LCL lines were a generous gift from Marie Bleakley, FHCRC. B-LCL lines were cultured for fewer than 10 passages in CTL medium and split twice weekly. Cell lines were not authenticated, and were tested for *Mycoplasma* monthly while in culture.

Antigen-presenting cells

Autologous B cells were isolated from PBMCs using positive selection with magnetic beads coated with antibodies recognizing CD19 (Miltenyi; cat. 130-050-301) according to the manufacturer's instructions (Miltenyi). B cells were cultured for 7 days in B-cell media composed of IMDM media (Life Technologies) supplemented with 10% human serum (in house), penicillin (100 U/mL; Life Technologies), and streptomycin (100 μg/mL; Life Technologies), 2 mmol/L L-glutamine (Life Technologies), and IL4 (200 U/mL; PeproTech) in the presence of 3T3 cells expressing human CD40L as described. B cells were then restimulated with irradiated (5,000 Gy) 3T3 expressing human CD40L cells, and fresh medium containing IL4 was added every 3 days. B cells were used in assays at day +3 after stimulation. For

KRAS-specific T cells, we used a B-LCL cell line (CLC) that is HLA-DRB1*11:04 as APCs in some experiments.

mRNA expression

RNA expression targeted to the endosome was carried out using the method described by the Sahin group (26), where antigens are targeted to the endosome by fusion of the antigen to class I MHC sorting signals. The mRNA expression construct pJV57 (27) was constructed by gene synthesis (GeneArt, Life Sciences), which contained a T7 promoter fused to the N-terminal 25 amino acids of the human HLA-B gene, followed by a BamHI restriction site, the coding sequence of enhanced GFP, an AgeI restriction site, the C terminal 55 amino acids of the human HLA-B gene, followed by the human beta-globin untranslated region followed by a 30-nucleotide poly-A tail and then a SapI restriction site directing cleavage in the poly-A tail. pJV126 was cloned by ligating the following into AgeI/BamHI digested pJV57: annealed oligonucleotides (Ultramers, Integrated DNA Technologies) encoding *Her2* amino acids 760–787 flanked by a 5′ AgeI and 3′ BamHI site. pJV127 was made by ligating annealed oligonucleotides (Ultramers, Integrated DNA Technologies) encoding *Her2* amino acids 760–787 flanked by a 5′ AgeI and 3′ BamHI site containing the YVMA tandem duplication.

pJV128 and pJV129 were synthesized in an analogous manner, with the first 25 amino acids of *KRAS* or the first 25 amino acids of *KRAS* with the G12V substitution, respectively.

pJV126 and other plasmids based on JV57 were linearized with SapI (Thermo Fisher), and mRNA was *in vitro* transcribed using the Highscribe T7 ARCA mRNA kit (New England Biolabs) and purified by lithium precipitation according to the manufacturer's instructions.

For RNA transfection, B cells or B-LCL were harvested, washed 1× with PBS, and then resuspended in Opti-MEM (Life Technologies) at 30×10^6 cells/mL. IVT RNA (10 μg) was aliquoted to the bottom of a 2-mm gap electroporation cuvette, and 100 μL of APCs were added directly to the cuvette. The final RNA concentration used in electroporations was 100 μg/mL. Electroporations were carried out using a BTX-830 square wave electroporator: 150 V, 20 ms, and 1 pulse. Cells were then transferred to B-cell medium supplemented with IL4 for 16 hours prior to cocultures (28).

ELISA assays

ELISA assays were performed by incubating 50,000 T cells in 96-well round-bottom plates with 100,000 autologous B cells or B-LCL lines pulsed with specific concentrations of peptides in RPMI (Gibco) supplemented with 5% heat-inactivated fetal bovine serum. IFNγ in supernatants was diluted 1:1, 1:10, and 1:100 and quantitated using human IFNγ ELISA kit (eBioscience) in technical duplicate or triplicate. HLA-blocking experiments were carried out by adding anti–class I (20 μg/mL; BioLegend; cat 311411), anti–HLA-DR (BioLegend clone L243, cat 307611), or HLA-DQ (Abcam, clone spv-l3, cat. ab23632) to the APCs 1 hour prior to adding peptide.

ELISpot assays

ELISpot assays were performed by incubating 20,000 to 100,000 T cells with 200,000 autologous B cells pulsed with 20 μg/mL of each peptide in CTL medium overnight using the human IFNγ ELISpot-Pro kit (Mabtech) according to the manufacturer's instructions.

Intracellular cytokine staining assays

PBMCs (100,000) were incubated with autologous B cells (100,000) pulsed with the indicated peptides (20 μg/mL) in the presence of brefeldin A (GolgiPlug, BD Biosciences) and then fixed and permeabilized using the BD intracellular staining kit (BD Biosciences) and analyzed using a FACS Canto2 flow cytometer.

Identification of T-cell receptor sequences

Total RNA was extracted from T-cell lines with the RNeasy Plus Mini Kit (Qiagen). RACE-ready cDNA was generated from RNA using the SMARTer RACE 5′/3′ Kit (Clontech) according to the manufacturer's protocol. CloneAmp HiFi PCR Premix (Clontech) was used to amplify 3′ cDNA fragments. Gene-specific primers (Human TCR Cbeta1 Reverse: 5′-CCA CTT CCA GGG CTG CCT TCA GAA ATC-3′; Human TCR Cbeta2 Reverse: 5′-TGG GAT GGT TTT GGA GCT AGC CTC TGG-3′; Human TCR Calpha Reverse: 5′-CAG CCG CAG CGT CAT GAG CAG ATT A-3′) were designed to detect alpha and beta TCR bands (1 Kb). The 3-step touchdown PCR reaction went through 35 cycles of 95°C for 10 seconds, 60°C for 15 seconds (decreasing by 0.2°C each cycle), and 72°C for 1 minute. The fragments were run on a 1% agarose gel and purified (QIAquick Gel Extraction Kit, Qiagen) for pENTR Directional TOPO cloning (Thermo Fisher). DNA was extracted (QIAprep Spin Miniprep Kit, Qiagen) from 8 to 10 clones for each TCR alpha and beta, followed by Sanger sequencing (JV298: 5′-TCG CTT CTG TTC GCG CGC TT-3′; JV300: 5′-AAC AGG CAC ACG CTC TTG TC-3′). TCR sequencing included in this paper will be available online at https://www.adaptivebiotech.com/products-services/immunoseq/immunoseq-analyzer/.

T-cell receptor vector construction

TCR construction was in the vector PRRL (29) further modified by introducing six point mutations into the start codon and putative promoter region of the woodchuck hepatitis virus X protein as described (30), with the TCR beta gene preceding the TCR alpha gene separated by a P2A translational skip sequence. Cysteine residues were introduced to facilitate pairing of introduced TCR chains as described (31). Specific variable regions and CDR3 sequences are shown in Supplementary Table S1. Codon-optimized DNA fragments containing the *TRBV* and CDR3 and *TRBJ* sequences followed by *TCRB* sequence with a cysteine substituted at residue 57 followed by a P2A skip sequence and the *TRAV* and CDR3 sequences followed by *TRAJ* and *TRAC* sequences were synthesized as a genestring (Life Sciences) and cloned using the NEBuilder cloning kit (New England Biolabs) into the lentiviral vector PRRL-SIN linearized with PstI and AscI (Thermo Fisher) and the sequence verified. One week after transduction, cells were sorted based on Vb expression using specific antibodies (Supplementary Table S1) and expanded as described above. T cells were used in assays or cryopreserved on day 14 after expansion.

CRISPR-Cas9–mediated gene deletion

CRISPR-Cas9 RNP targeting the first exon of the TCR alpha constant region were created as previously described (32) by mixing equal volumes of 80 μmol/L TracRNA (IDT) with 80 μmol/L of the gRNA AGAGTCTCTCAGCTGGTACA (25) in duplex buffer (IDT) and heated to 95°C in a heating block for 5 minutes and allowed to slowly cool. The resulting 40 μmol/L duplexed RNA was mixed with an equal volume of 24 μmol/L

Cas9 protein (IDT) and 1/20 volume of 400 μmol/L Cas9 electroporation enhancer (IDT) and incubated at room temperature for 15 minutes prior to electroporation.

On day 0, $CD4^+$ T cells were isolated from cryopreserved healthy human donor PBMC from 4 patients who provided informed consent on an IRB-approved protocol by negative immune selection using the EasySEP human $CD4^+$ isolation kit (Stemcell Technologies) and stimulated with anti-CD3/anti-CD28 microbeads at a 3:1 bead:cell ratio (Dynabeads, Invitrogen) in the presence of IL2 (50 U/mL) and IL7 (5 ng/mL) in CTL media for 2 days. Also, on day 0, Lenti-X cells (Clontech) were transiently transfected with the TCR vector, as well as psPAX2 (Addgene plasmid no. 12260) and pMD2.G (Addgene plasmid no. 12259) packaging plasmids. On day +2, magnetic beads were removed, and 1×10^6 cells were nucleofected using a Lonza 4D nucleofector in 20 μL of buffer P3 using program EH-115. Cells were allowed to rest for 4 hours in media prior to lentiviral transduction. Lentiviral supernatant was harvested from Lenti-X cells, filtered using 0.45-μm polyethersulfone (PES) syringe filters (Millipore), and 900 μL added to 50,000 activated T cells in a 48-well tissue culture plate. Polybrene (Millipore) was added to a final concentration of 4.4 μg/mL, and cells were centrifuged at 800 × *g* and 32°C for 90 minutes. Viral supernatant was replaced 16 hours later with fresh CTL supplemented with IL2 (50 IU/mL) and IL7 (5 ng/mL). Half-media changes were then performed every 48 to 72 hours using CTL supplemented with IL2 and IL7. Transduced T cells were sorted on day +7 or +8 of stimulation using antibodies specific to the transduced TCRVb (Supplementary Table S1) and grown in a rapid expansion protocol described above for 12 to 14 days prior to conducting of immune assays.

Nucleic acid preparation for exome capture and RNA-seq

Nontumor DNA was isolated from nonadjacent lung for patients 1490, 1238, and 1139. Blood was used as nontumor DNA for patients 511 and 1347. Single-cell suspensions derived from tumor, lung tissue, or PBMCs were processed with the Qiagen DNA/RNA AllPrep Micro kit to isolate DNA for exome capture, with RNA reserved for subsequent RNA-seq profiling. In addition to DNA isolated from the initial tumor resection, a PDX was established from the tumor of patient 1347, and the PDX tumor was used for DNA and RNA preparation. Genomic DNA concentration was quantified on an Invitrogen Qubit 2.0 Fluorometer (Life Technologies-Invitrogen) and Trinean DropSense96 spectrophotometer (Caliper Life Sciences).

TCR Vβ sequencing

DNA from clinical samples was isolated using the Qiagen DNeasy or Qiamp micro DNA kits according to the manufacturer's instructions. TCRB sequencing was carried out using the human TCRB sequencing kit (Adaptive Biotechnologies) following the manufacturer's instructions and sequenced using a MiSeq (FHCRC Genomics core) with data analysis carried out by Adaptive Biotechnologies software.

Whole-exome sequencing

Exome-sequencing libraries were prepared using the Agilent SureSelectXT Reagent Kit and exon targets isolated using the Agilent All Human Exon v6 (Agilent Technologies). Genomic DNA (200 ng) was fragmented using a Covaris LE220 focused-ultrasonicator (Covaris, Inc.), and libraries were prepared and captured on a Sciclone NGSx Workstation (PerkinElmer). Library size distributions were validated using an Agilent 2200 TapeStation. Additional library QC, blending of pooled indexed libraries, and cluster optimization was performed using Life Technologies' Invitrogen Qubit 2.0 Fluorometer.

The resulting libraries were sequenced on an Illumina HiSeq 2500 using a paired-end 100 bp (PE100) strategy. Image analysis and base calling was performed using Illumina's Real-Time Analysis v1.18 software, followed by "demultiplexing" of indexed reads and generation of FASTQ files using Illumina's bcl2fastq Conversion Software v1.8.4 (http://support.illumina.com/downloads/bcl2fastq_conversion_software_184.html). Read pairs passing standard Illumina quality filters were retained for further analysis, yielding an average of 65.2M read pairs for the tumors and 64.4M read pairs for the normals among samples reported here. Paired reads were aligned to the human genome reference (GRCh37/hg19) with the BWA-MEM short-read aligner (33, 34). The resulting alignment files, in standard BAM format, were processed by Picard 2.0.1 and GATK 3.5 (35) for quality score recalibration, indel realignment, and duplicate removal according to recommended best practices (36).

To call somatic mutations from the analysis-ready tumor and normal BAM files, we used two independent software packages: MuTect 1.1.7 (21) and Strelka 1.0.14 (22). Variant calls from both tools, in VCF format, were annotated with Oncotator (37). Annotated missense somatic variants were combined into a single summary for each sample as follows. First, any mutation annotated as "somatic" but present in dbSNP was removed if it was also not present in COSMIC or its minor allele frequency was greater than 1% (according to the UCSC Genome Browser snp150 Common table). Variants supported by both variant callers were retained, and those supported by only one variant caller were subject to manual inspection.

RNA-seq data processing

For patient 1347, direct measurements of RNA expression for candidate mutations were performed using tumor cells from the PDX. An RNA-seq library was prepared from total RNA using the TruSeq RNA Sample Prep v2 Kit (Illumina, Inc.) and a Sciclone NGSx Workstation (PerkinElmer). Library size distributions were validated using an Agilent 2200 TapeStation (Agilent Technologies). Additional library QC, blending of pooled indexed libraries, and cluster optimization was performed using Life Technologies' Invitrogen Qubit 2.0 Fluorometer (Life Technologies-Invitrogen). The library was sequenced on an Illumina HiSeq 2500 to generate 61 M read pairs (two 50 nt reads per pair). Reads were first aligned to the mouse reference assembly (mm9) to remove reads from the mouse rather than the engrafted tumor. Remaining reads were aligned to a human RefSeq-derived reference transcriptome with RSEM 1.2.19 (38) to derive abundances for each gene in TPM units.

Statistical analysis

Statistical analysis was conducted using GraphPad Prism 7.0. ELISpot data were analyzed by one-way ANOVA with the Sidak correction for multiple comparisons. Enrichment of TCR Vβ templates within tumor tissue was evaluated using the Fisher exact test.

Data availability

Exome sequencing and RNA-seq of patients 1347, 1238, 1139, and 1490 are uploaded to dbGaP as allowed by the IRB (patient

511 did not consent to database upload), accession number phs001805.v1.p1. Processed TCR sequencing data are available through a public immuneACCESS project in the immunoseq analyzer (https://www.adaptivebiotech.com/products-services/immunoseq/immunoseq-analyzer; Adaptive Biotechnologies). Plasmids and plasmid sequences have been deposited in Addgene (www.addgene.org).

Results

We obtained tumor specimens from 4 patients with lung adenocarcinoma and 1 patient with squamous cell carcinoma (Table 1), and performed whole-exome sequencing of tumor and normal germline DNA. Protein-coding variants were ranked by variant allele frequency and mRNA expression. Based on these results and feasibility, 20 to 57 mutations were selected per patient for analysis of T-cell responses (Table 1; Supplementary Table S2). We initially performed a screening assay for T-cell responses to candidate neoantigens by stimulating PBMCs with a pool of overlapping 20-amino acid peptides encompassing each of the mutations and evaluating reactivity by IFNγ ELISpot assay (Fig. 1A). T-cell cultures with reactivity above background to a candidate neoantigen were then reassayed for IFNγ production in response to purified 27-mer peptides corresponding to the mutant and wild-type sequences (Fig. 1B). In total, T-cell responses to 21 of the 238 neoantigens (8.8%) screened were detected and were significantly elevated compared with wild-type peptide responses ($P < 0.05$). ELISpot assays using peptides can have both false-positive and false-negative results, and additional weak responses to mutations in *KRAS* and *Her2*-ITD were observed and did not meet the cutoff criteria but were selected for further study because of the important role of these mutations in oncogenesis.

We further characterized potential neoantigen-reactive T cells expanded from the blood from patients 1490 and 1347, from whom additional cryopreserved samples and TILs were available. PBMCs from these patients were stimulated with purified 27-mer peptides for each of the mutants that elicited a response (meeting the criteria above), and following restimulation, IFNγ$^+$ cells were sorted and expanded by limiting dilution cloning. We isolated a single CD4$^+$ clone reactive to the mutation GUCY1A3 and two different CD4$^+$ clones reactive to a mutation in SREK1 from patient 1490. Each of these clones showed specificity for the mutant relative to the wild-type peptides (Fig. 2A). Other isolated T-cell clones were reactive to mutant SREK1 peptide, but the response was similar to that seen with SREK1 wild-type peptide (Supplementary Fig. S1), potentially explaining the reactivity to the wild-type peptide observed in the screening ELISpot (Fig. 1B). We were unable to isolate T-cell lines or clones specific for other neoantigens from patients 1490 and 1347. Two clones specific for SREK1 with different TCRVβ sequences were detected in the initial tumor resection (8/24,095 templates) and were enriched relative to the nonadjacent lung tissue from the same resection (1/62,424 templates in nonadjacent lung, $P = 0.0002$). The GUCY1A3 TCRVβ was not detected in the tumor resection sample or the lung. These observations suggested that CD4$^+$ T cells reactive to neoantigens can be isolated from the blood, and in one case, these cells can localize to tumor tissue. It is possible that the inability to isolate additional neoantigen-specific T cells could reflect T-cell exhaustion or limitations of our methods to expand such cells.

For patients 1490 and 1347, a TIL culture was made from the initial resection sample by culture of tumor fragments in high-dose IL2 (25), and we assayed the TILs for neoantigen reactivity by ELISpot and intracellular IFNγ with 20-mer overlapping peptides described previously. No reactivity was found to screened antigens from patient 1347, but CD8$^+$ T cells in the TILs from patient 1490 were reactive to a mutation in PWP2 (Fig. 2B). The TCRVβ expressed by sorted *PWP2*-reactive CD8$^+$ T cells was identified, and the frequency of the *PWP2*-reactive TCRVβ was determined in the initial tumor resection sample, nonadjacent lung, and after culturing of TILs. The TCRVβ sequence was enriched in the tumor resection relative to the nonadjacent lung (0.2%, 54/24,095 templates vs. 0.03%, 18/62,424 templates, $P < 0.0001$) and was further enriched by TIL culture (4.8% of templates; Fig. 2C). A *PWP2*-reactive T-cell line was expanded from TILs after IFNγ capture, and reactivity to the mutant, but not wild-type 10-mer peptide, was confirmed (Fig. 2D). TCRVβ sequencing identified the TCRVβ clonotype following stimulation of peripheral blood at a frequency of 0.07% of TCRVβ templates, which may have been too low for detection by the IFNγ ELISpot assay. Thus, T cells with different specificities may be isolated from cultured TIL products and blood, potentially due to the insensitivity of the methods or the difficulty in expanding T cells that may be functionally impaired due to the presence of chronic antigen.

The majority of potential neoantigen-specific T cells identified in blood or tumor by our analysis recognized private, patient-specific mutations consistent with prior studies in other cancers (2, 4, 7, 16). The weak T-cell responses in the blood to the recurrent driver mutation *KRAS*^{G12V} in patient 1139 and *Her2*-ITD in patient 1238 did not reach statistical significance, but given the importance of these proteins to the malignant phenotype, were worthy of additional efforts to characterize the specificity. We stimulated PBMCs from patient 1139 twice with *KRAS*^{G12V} peptide, and then identified and sorted IFNγ-secreting CD4$^+$ T cells, and expanded these T cells in limiting dilution cultures. Four T-cell cultures were obtained that secreted IFNγ specifically in response to low concentrations of *KRAS*^{G12V} peptide but not to the corresponding wild-type KRAS peptide. TCRVβ sequencing revealed that these represent monoclonal populations with three distinct TCRVβ clonotypes, referred to as clones 3, 5, and 9 (Fig. 3A). IFNγ production to *KRAS*^{G12V} was partially blocked by anti–HLA-DR but not anti–HLA-DQ, suggesting restriction by HLA-DR (Fig. 3B). The patient's HLA genotype was HLA-DRB1*11:04/13:01, HLA-DQB1*03:01/06:03. All three T-cell clones showed reactivity with LCL cell lines expressing HLA-DRB1*11:01 or 11:04 pulsed with KRAS^{G12V} peptide, but not peptide-pulsed LCL expressing DQB1*03:01 or DQB1*06:01 in the absence of HLA-DRB1*11, indicating HLA restriction by HLA-DRB1*11 (Fig. 3C). No *KRAS*^{G12V}-specific TCRVβ clonotypes were detected in the resection specimen or nonadjacent lung from the tumor, which were each sequenced to a depth of 10,000 TCRVβ templates.

Reactivity of the *KRAS*^{G12V}-specific T-cell clones to APCs pulsed with wild-type peptide at very high peptide concentrations was observed. Antigens are normally presented to CD4$^+$ T cells after endogenous processing in the endosome (26). Thus, to determine whether the *KRAS*^{G12V}-reactive T-cell clones recognized processed antigen, HLA-matched B-LCLs were transfected with mini-gene constructs encoding either *KRAS*^{G12V} or wild-type *KRAS* with endosomal targeting sequences. Each of the three clones specifically recognized cells expressing *KRAS*^{G12V} but not wild-type *KRAS* sequences (Fig. 3D), indicating specificity for endogenously processed neoantigen. We next obtained the *KRAS*^{G12V}-specific

Table 1. Characteristics of patients in this study mSNVs—missense SNVs

Patient #	Age at blood donation	Diagnosis	Smoking history	Stage at resection	Stage at blood donation	Time between resection and blood donation	Prior treatments	Treatment at blood donation	mSNVs	Mutations screened
511	73	Adeno carcinoma	Yes	IV lymph node	IV	30 months	Carboplatin/ pemetrexed	Pemetrexed	505	46
1490	62	Adeno carcinoma	Yes	IB lung tumor	III	13 months	None	Carboplatin, paclitaxel, radiation	130	46
1347	64	Squamous cell Carcinoma	Yes	IIB lung tumor	No evidence of disease	10 months	Carboplatin/Paclitaxel	None	65	57
1139	69	Adeno carcinoma	Yes	Stage IV lung tumor	IV	27 months	Carboplatin/ pemetrexed	Nivolumab	388	48
1238	68	Adeno carcinoma	No	IIIA lung tumor	IV	23 months	Cisplatin/pemetrexed, afatinib, pembrolizumab, docetaxel/ ramicirumab	Ramicirumab	34+ Her2 ITD	20+ Her2 ITD

TCRVβ and Vα sequences from T-cell clones by 5′ RACE, and constructed lentiviral vectors encoding these TCRs. Transduction of the TCRs from clones 3 and 9 into $CD4^+$ T cells from two normal donors conferred specificity for target cells pulsed with peptides or those expressing $KRAS^{G12V}$ but not wild-type *KRAS* sequences (Fig. 3E–G). In these experiments, donor T cells underwent CRISPR-Cas9–mediated disruption of exon 1 of the endogenous TCRα constant region gene (*TRAC*) prior to gene transfer of the transgenic TCR (Supplementary Fig. S2A) to minimize background activation of these cells with allogeneic APCs (Supplementary Fig. S2B). As observed for the original T-cell clones, T cells engineered with the $KRAS^{G12V}$-specific TCRs exhibited recognition of target cells pulsed with low concentrations of mutant peptide that were >2 $\log_{10}$ lower than the wild-type KRAS peptide.

Patient 1238 exhibited a weak $CD4^+$ T-cell response to the recurrent *Her2* exon 20 insertion that creates an in-frame duplication of the amino acids YVMA (*Her2*-ITD; Supplementary Fig. S3A; Fig. 1B). We took the same approach used to isolate $KRAS^{G12V}$-specific T cells and successfully isolated *Her2*-ITD–specific $CD4^+$ T-cell lines. Analysis of multiple T-cell lines by TCRVβ sequencing revealed a single recurrent TCRVβ clonotype present in all 10 T-cell lines (Supplementary Fig. S3B), which was nearly clonal in one T-cell line (#35). This line recognized the mutant *Her2*-ITD peptide at low peptide concentrations but not the corresponding wild-type Her2 peptide (Fig. 4A), and reactivity was completely blocked by anti–HLA-DQ, but not anti–HLA-DR or anti–class I (Fig. 4B). Consistent with the blocking data, the T cells reacted only with *Her2*-ITD peptide–pulsed B-LCL lines expressing HLA-DQB1*05:01 and 05:02, suggesting HLA restriction by HLA DQB1-05 (Fig. 4C). These T cells also specifically recognized MHC class II^+ cells transfected with mutant but not wild-type *Her2* sequences targeted to the endosome (Fig. 4D). TCRVβ and Vα sequences of the *Her2*-ITD–specific line were obtained by 5′ RACE. Lentiviral gene transfer of the TCR sequences, following the disruption of the endogenous TCRα by CRISPR-Cas9–mediated gene deletion, conferred specificity to the Her2-ITD peptide and MHC class II^+ cells transfected with the mutant, but not wild-type, *Her2* sequences (Fig. 4E and F). The expression of the transferred TCRs, measured by staining with a Vβ2-specific antibody, was improved by CRISPR-mediated deletion of the endogenous TCRα constant region gene *TRAC* (Supplementary Fig. S4), consistent with prior reports showing that downregulation of the endogenous TCR results in greater expression of the gene-transferred TCR (39).

TCRVβ deep sequencing of the initial lung resection sample from patient 1238 identified the *Her2*-ITD–specific TCRVβ clonotype in 3 of 20,179 templates in the tumor resection. Despite 5-fold deeper sequencing of the nonadjacent lung tissue from the resection, no *Her2*-ITD–specific clonotype was observed, showing enrichment of *Her2*-reactive $CD4^+$ T cells in the tumor (Fig. 4G; $P = 0.004$ for enrichment). The presence of *Her2*-ITD–specific $CD4^+$ T cells in the blood 2 years after tumor resection is consistent with these cells being part of a persistent memory T-cell response to the tumor.

Discussion

We set out to characterize whether preexisting T-cell responses could be expanded from the blood of five patients with NSCLC and identified responses to 8.8% of screened mutations. Neoantigen-specific T-cell clones could be isolated for four different mutations in three patients, and in all cases, the T-cell clones were $CD4^+$, which has been seen previously in melanoma (16, 17, 40). For two antigens (SREK and Her2-ITD) from two different patients, neoantigen-specific $CD4^+$ TCRVβ clonotypes had low detection in tumor samples and were enriched relative to nonadjacent lung samples. The clinical significance of these responses is unknown, but the data are consistent with at least a subset of neoantigen-specific $CD4^+$ T cells detected in the blood as part of an active but ineffective immune response to NSCLC. We cannot exclude the possibility that some of the other responses in blood represent *in vitro* priming of naïve T cells or cross-reactive T-cell responses to unrelated antigens rather than a memory immune response to the cancer. A report has shown that similarly low-frequency neoantigen-specific $CD4^+$ T cells can be isolated directly from the tumors of patients with gastrointestinal and ovarian tumors, and these cells express PD-1, suggesting activation in the tumor microenvironment (41). However, these observations do not establish the functional importance of these or other neoantigen-specific $CD4^+$ T-cell responses in the immune response to NSCLC relative to other cell types, which still remains unknown.

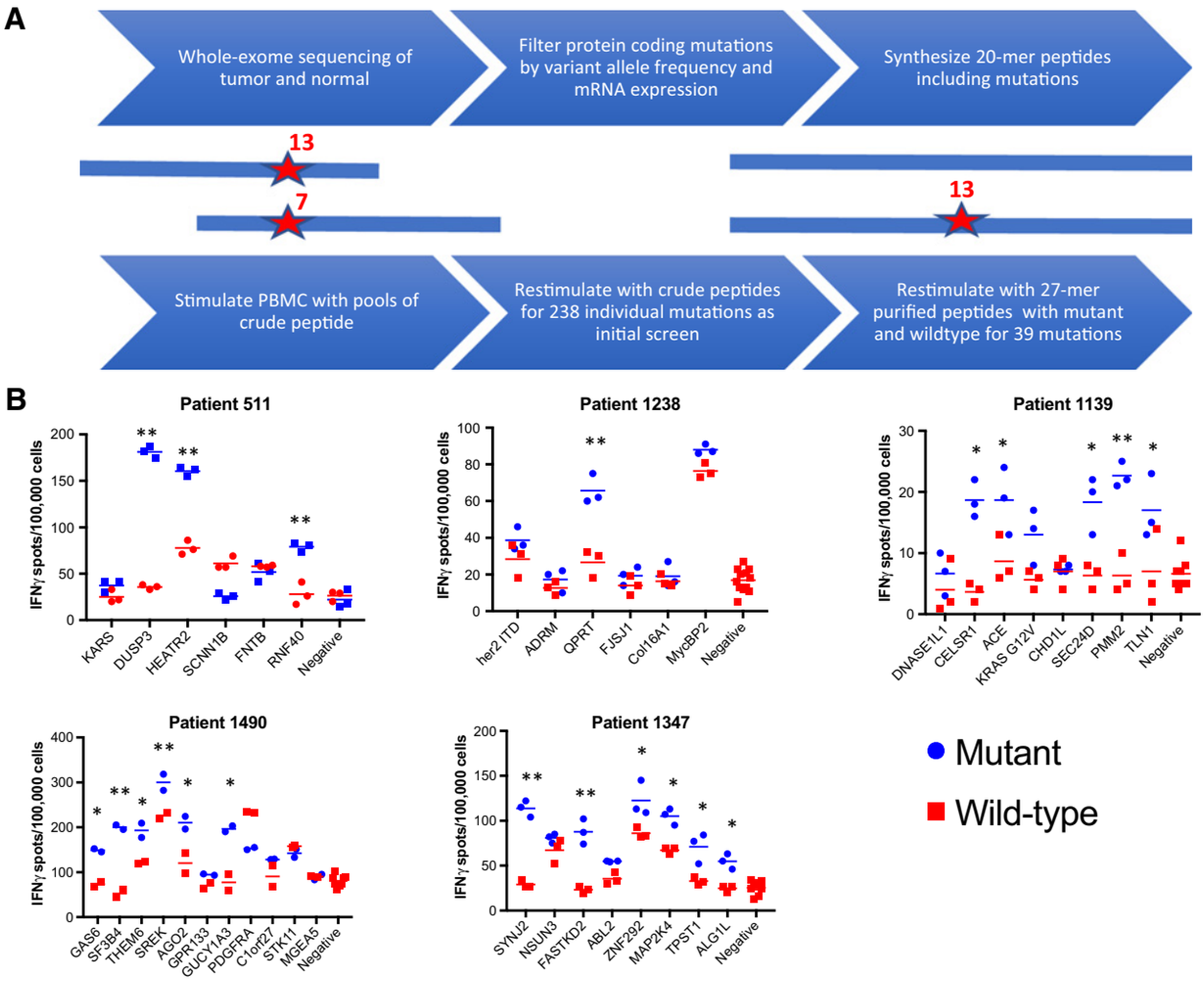

Figure 1.

Detection of neoantigen-reactive T cells in lung cancer patients. **A,** Schematic for detecting neoantigen-reactive T cells. **B,** PBMCs from 5 different lung cancer patients were stimulated with pools of mutant peptides (1 μg/mL for each peptide). IFNγ-secreting cells from stimulated cultures were quantitated by ELISpot after incubation with single-mutant or wild-type peptides (10 μg/mL). All experiments included 2 or 3 technical replicates. *, $P < 0.05$ for comparison with negative and $P < 0.05$ for comparison of mutant to wild-type by one-way ANOVA; **, $P < 0.0005$ for both comparisons by one-way ANOVA. Bars, mean.

Previous attempts to identify and isolate neoantigen-specific T-cell responses in lung cancer have focused on $CD8^+$ T cells, using MHC tetramer technology, or stimulation of blood with short peptides based on predicted binding to class I MHC. Our approach using long peptides could, in theory, expand both $CD4^+$ and $CD8^+$ T-cell responses (42), but may be less effective for expanding $CD8^+$ T-cell responses due to the need for additional cellular peptide processing for presentation. A relative lack of $CD8^+$ neoantigen-specific T cells identified in peripheral blood could reflect a difference in the frequency of these cells in the tumor relative to the blood, or a difference in their ability to expand and be detected with the functional assay used in our experimental protocol. The culture of TILs from patient 1490 led to expansion of $CD8^+$ T-cell specific for the *PWP2* mutation, but not $CD4^+$ T cells specific for the *SREK1* mutation. This is consistent with a report suggesting that multiple neoantigen-specific $CD4^+$ responses expanded from unmanipulated tumors are not detected following tumor fragment culture, and reveals the limitations of current approaches for assessing neoantigen-specific T cells (41).

We chose mutations agnostic of HLA type and computational prediction algorithms for predicting peptide binding to class II MHC (43). When we include our prior reported class II–restricted $BRAF^{V600E}$-restricted $CD4^+$ T-cell response (27), only one of the three validated $CD4^+$ T-cell responses to recurrent driver mutations is predicted to have even weak binding to the restricting MHC allele (best predicted binding 134 nmol/L for $KRAS^{G12V}$, 574 nmol/L for *Her2*-ITD, and 1,442 nmol/L for $BRAF^{V600E}$ using NetMHCIIpan). Together, these data suggest that NetMHCIIpan is not yet sufficiently sensitive to screen MHC class II–restricted neoantigens, although we cannot make inferences about better-studied class II MHC alleles or other prediction algorithms.

We also report T-cell responses to driver mutations in lung cancer. The neoantigen created by the $KRAS^{G12V}$ mutation recognized by the patients' $CD4^+$ T cells is found in 4% of NSCLC, 10% of colorectal cancer, 30% of pancreas cancer, and 8% of ovarian

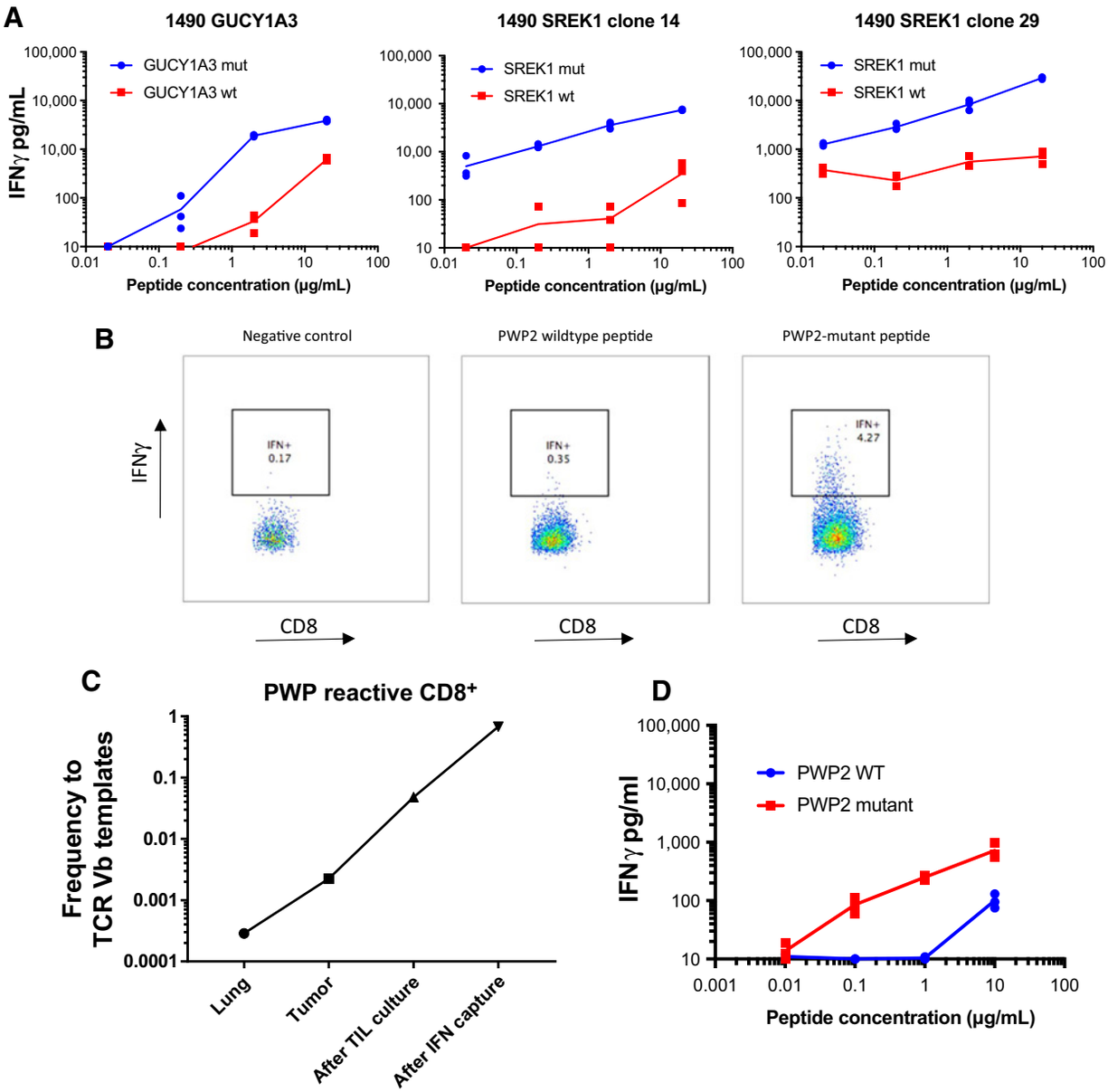

Figure 2.

Neoantigen-specific CD4$^+$ T cells detected in blood and CD8$^+$ T cells detected in TIL cultures. **A,** Monoclonal CD4$^+$ T-cell lines from patient 1490 reactive with a mutation in *SREK1* and *GUCY1A3* were expanded *in vitro* and then incubated with autologous B cells and the indicated concentration of mutant and wild-type peptide. IFNγ secretion was measured by ELISA. **B,** TILs from the tumor resection of patient 1490 were incubated with long peptides containing mutant (VVGSKDMSTWVFGTERWDNLIYYALGG) or wild-type (VVGSKDMSTWVFGAERWDNLIYYALGG) sequences from PWP2, and IFNγ secretion was measured by interferon capture (**C**) TCRVβ clonotype frequency of PWP2-reactive CD8$^+$ TCRVβ in nonadjacent lung, tumor, following TIL culture, and following IFNγ capture of TIL product. **D,** IFNγ release was measured when the PWP2-reactive T-cell line was incubated with autologous B cells and the indicated concentrations of mutant (TERWDNLIYY) and wild-type (AERWDNLIYY) PWP2 peptide.

cancer (8), and the HLA-DR11–restricting allele is found in 18% of patients (44). A second CD4$^+$ T-cell response specific for the Her2 exon 20 insertion found in a different patient is present in 2% to 4% of NSCLC (9), and the HLA-DQ5–restricting allele is found in 30% of patients (44). Combined with our previous description of a *BRAF*^{V600E}-specific CD4$^+$ T-cell response in melanoma (27) and the work of others in different cancers (41, 45), these findings suggest that CD4$^+$ T cells specific for recurrent driver mutations might be more common in human cancer than previously perceived. The finding that recurrent cancer mutations predicted to be presented to CD4$^+$ T cells on class II MHC are underrepresented across multiple tumor types lends support to the hypothesis that driver mutation–specific CD4$^+$ T cells could have a functional role in tumor surveillance (12).

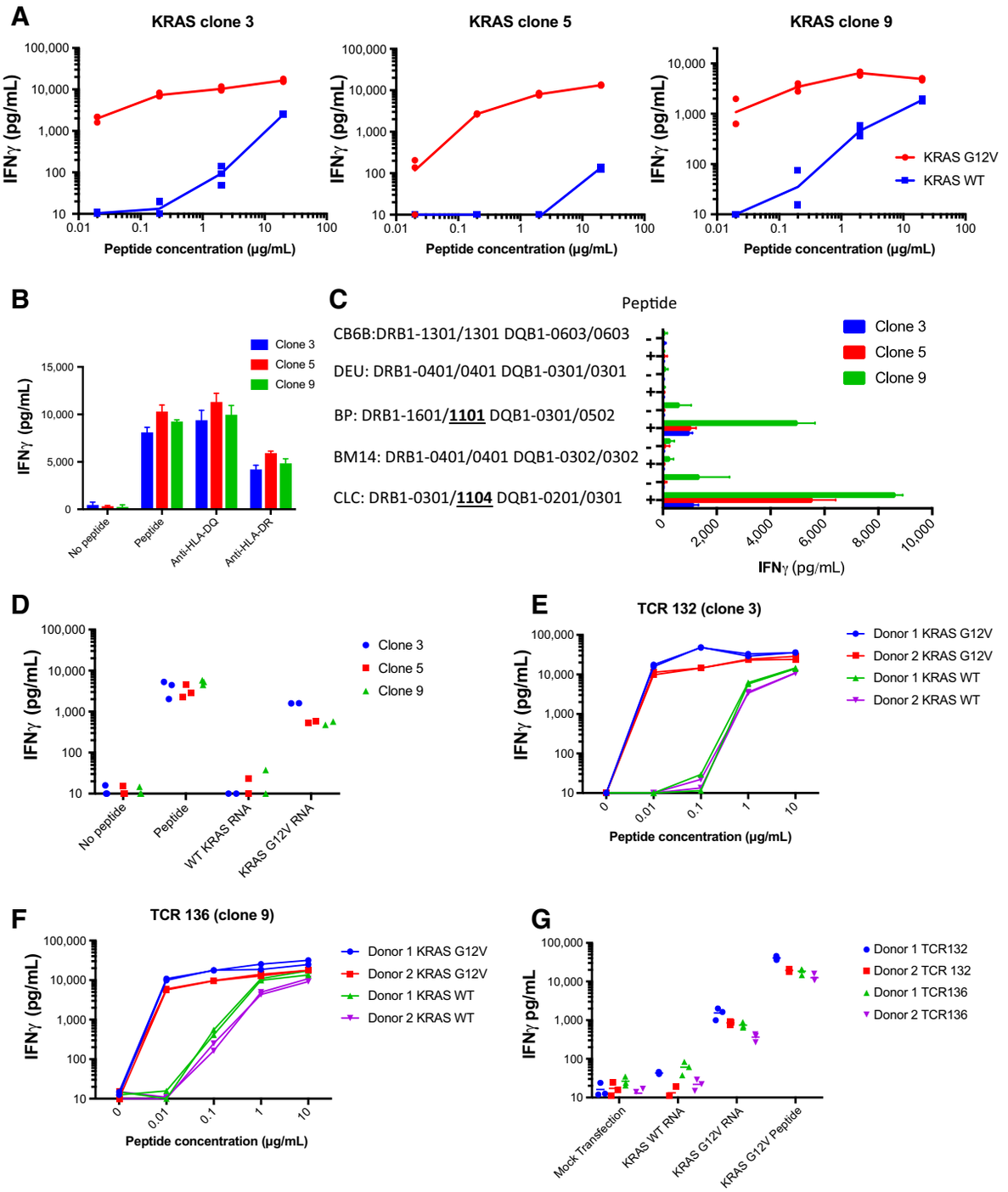

Figure 3.

T-cell clones specifically recognize *KRAS*^{G12V}. **A,** Three CD4$^+$ T-cell clones from patient 1139 were incubated in the presence of the indicated concentration of the N-terminal 26 amino acids of *KRAS* with either V12 (mutant MTEYKLVVVGAVGVGKSALTIQLIQ) or G12 (wild-type MTEYKLVVVGAGGVGKSALTIQLIQ), and IFNγ production was measured by ELISA. **B,** T-cell clones were incubated with *KRAS*^{G12V} peptide (1 μg/mL) in the presence of the indicated class II HLA-blocking antibodies (20 μg/mL), and IFNγ production was measured by ELISA. **C,** T-cell clones were incubated with B-LCL cell lines, which had been pulsed with *KRAS*^{G12V} peptide (1 μg/mL) and expressed individual class II HLA alleles shared with patient 1139 (HLA-DQB1*11:04/13:01 DQB1*03:01/06:03). **D,** T-cell clones were incubated with HLA-DRB1*11:04$^+$ LCLs pulsed with *KRAS*^{G12V} peptide (1 μg/mL) or transfected with RNA encoding wild-type or KRAS^{G12V} sequences, and IFNγ production was measured by ELISA. **E–G,** CD4$^+$ T cells from 2 normal donors were transduced with lentiviral vectors encoding T-cell receptor Vα and Vβ genes from T-cell clones #3 and #9 with concurrent CRISPR-mediated disruption of the endogenous TCRα and then incubated HLA-DRB1*1104$^+$ LCL cells pulsed with *KRAS*^{G12V} peptide or **G**) B-LCL cells transfected with mutant or wild-type *KRAS* sequences, and IFNγ production was measured by ELISA.

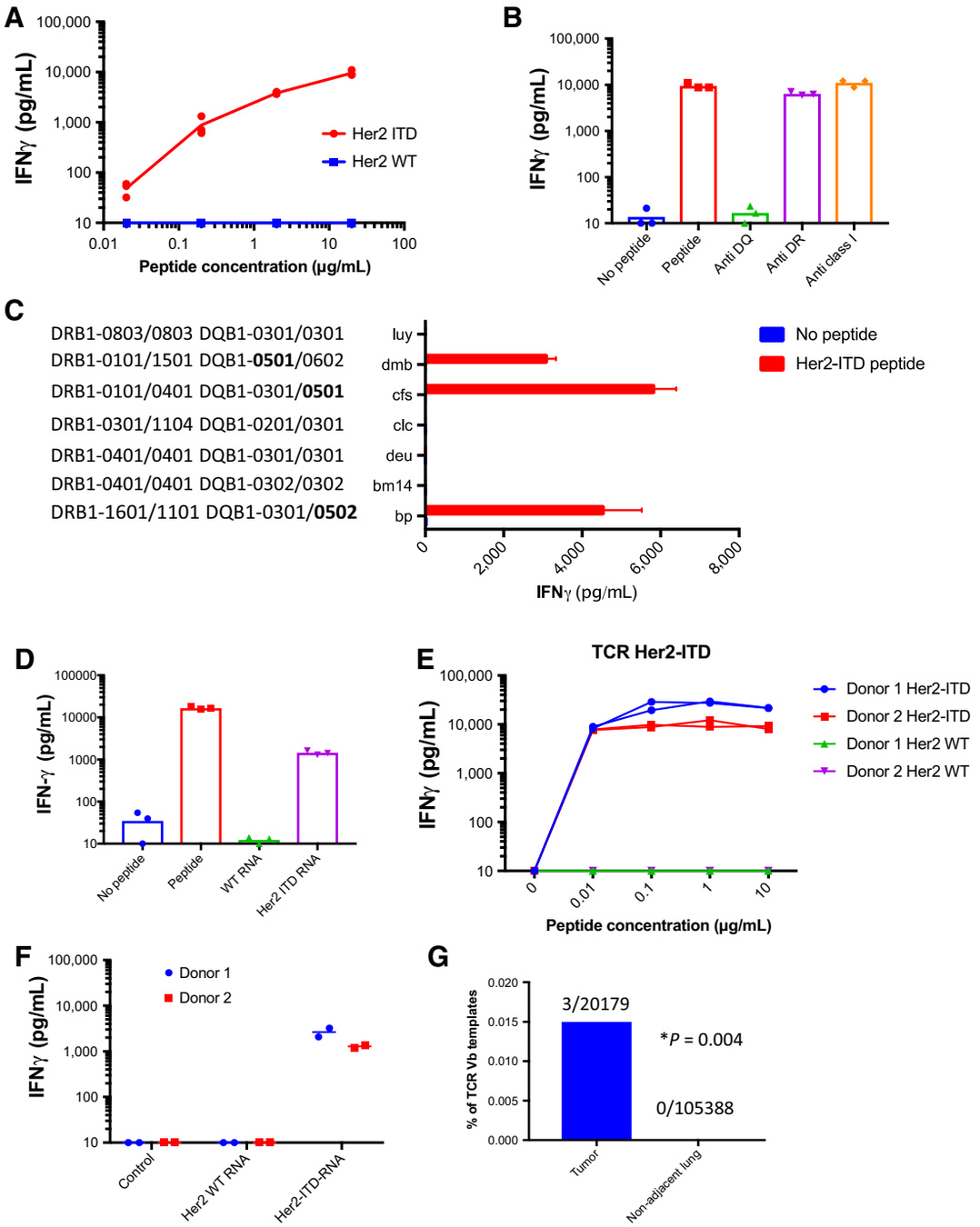

Figure 4.

CD4$^+$ T cells specific for the Her2 exon 20 insertion (Her2-ITD). **A,** A CD4$^+$ T-cell line from patient 1238 (50,000 cells) was cocultured with autologous B cells (100,000 cells) in the presence of the indicated concentration of Her2-ITD (SPKANKEILDEAYVMAYVMAGVGSPYVSRLLG) or the corresponding wild-type peptide (SPKANKEILDEAYVMAGVGSPYVSRLLG), and IFNγ production was measured by ELISA. **B,** The CD4$^+$ T-cell line from patient 1238 (50,000 cells) was incubated with Her2-ITD peptide in the presence of 100,000 autologous B cells the indicated class II MHC blocking antibodies. **C,** The CD4$^+$ T-cell line was incubated with autologous B cells pulsed with Her2-ITD peptide (10 μg/mL) or transfected with RNA encoding wild-type or *Her2*-ITD sequences. **D,** The CD4$^+$ T-cell line (50,000 cells) was incubated with Her2-ITD peptide (20 μg/mL) pulsed B-LCL cell lines (100,000 cells) expressing individual class II HLA alleles shared with patient 1238. **E** and **F,** CD4$^+$ T cells from two normal donors were transduced with TCR sequences obtained from Her2-ITD–specific T cells with concurrent disruption of the endogenous TCRα gene and 50,000 T cells were incubated with B-LCL cells (100,000) pulsed with Her2-ITD peptide or **F**) incubated with B-LCL cells transfected with wild-type or mutant Her-2 sequences, and INFγ production measured in the supernatant by ELISA. **G,** Tumor and nonadjacent lung were subjected to deep TCRVb sequencing and the Her2-ITD–specific Vβ was quantitated as a percentage of TCR Vβ templates $P = 0.004$ for enrichment in the tumor relative to lung by Fisher exact test.

Neoantigen vaccination strategies in murine models suggest that $CD4^+$ responses to neoantigens are more prevalent and potentially more effective in antitumor immunity than $CD8^+$ T-cell responses (15). A global analysis of immune subsets in a mouse model of tumor rejection highlighted changes in Th1 $CD4^+$ T cells distant to the tumor, and showed the ability of adoptive transfer of these $CD4^+$ T cells to confer antitumor immunity (14). Adoptive transfer of human $CD4^+$ T cells specific for a neoantigen resulted in a clinical response in a patient with cholangiocarcinoma (28), and early results from neoantigen vaccination trials that elicited predominantly $CD4^+$ T-cell responses support the clinical efficacy of these approaches (17, 40). Despite significant evidence pointing toward the importance of $CD4^+$ T-cell responses to neoantigens, many epithelial cancers lack class II MHC, and the precise mechanisms through which $CD4^+$ T cells mediate antitumor immunity remain to be fully elucidated.

The discovery of $CD4^+$ T-cell responses to neoantigens in NSCLC, including recurrent driver mutations in *KRAS* and *Her2*, suggests that augmenting responses to these antigens through vaccination or adoptive transfer of TCR gene–modified T cells could allow direct interrogation of whether such T-cell responses have a functional role in antitumor immunity. The isolation of TCRs specific for recurrent *KRAS* and *Her2* mutations that confer specificity upon gene transfer provides the foundation to examine the effect of augmenting $CD4^+$ T-cell immunity to neoantigens by adoptive transfer and potentially elucidate the mechanisms of $CD4^+$ T cells more broadly in human antitumor immunity.

Disclosure of Potential Conflicts of Interest

J.R. Veatch and S.R. Riddell have ownership interest in a patent related to this work. S.M. Lee reports receiving a commercial research grant from Juno Therapeutics. C.S. Baik reports receiving commercial research grants from Novartis, Pfizer, Spectrum, Blueprint Medicines, Daiichi Sankyo, AstraZeneca, Celgene, Roche/Genentech, Merck Sharp & Dohme, MedImmune, Mirati, GlaxoSmithKline, and Loxo Oncology and is a consultant/advisory board member for AstraZeneca and Novartis. S. Riddell reports receiving a commercial research grant from Juno Therapeutics, a Celgene company, has ownership interest (including stock, patents, etc.) in Celgene, and is a consultant/advisory board member for Juno Therapeutics, a Celgene company. No potential conflicts of interest were disclosed by the other authors.

Authors' Contributions

Conception and design: J.R. Veatch, A.M. Houghton, S.R. Riddell
Development of methodology: J.R. Veatch, S.R. Riddell
Acquisition of data (provided animals, acquired and managed patients, provided facilities, etc.): J.R. Veatch, B.L. Jesernig, J. Kargl, S.M. Lee, C. Baik, R. Martins, A.M. Houghton
Analysis and interpretation of data (e.g., statistical analysis, biostatistics, computational analysis): J.R. Veatch, M. Fitzgibbon, S.R. Riddell
Writing, review, and/or revision of the manuscript: J.R. Veatch, B.L. Jesernig, J. Kargl, S.M. Lee, C. Baik, S.R. Riddell
Administrative, technical, or material support (i.e., reporting or organizing data, constructing databases): J.R. Veatch, S.R. Riddell
Study supervision: S.R. Riddell

Acknowledgments

J.R. Veatch was supported by NIH grants T32 T32CA009515 and K12 CA076930-16A1 and a generous contribution from the Lembersky family. M. Fitzgibbon, J.R. Veatch, B.L. Jesernig, and S.R. Riddell were supported by a generous gift from the Bezos family. J. Kargl was supported by the following grant EU-FP7-PEOPLE-2012-IOF 331255. S.R. Riddell has received laboratory funding from and has equity interest in Juno Therapeutics, a Celgene company; and has served as an advisor for Adaptive Biotechnologies, Nohla, and Cell Medica.

The costs of publication of this article were defrayed in part by the payment of page charges. This article must therefore be hereby marked *advertisement* in accordance with 18 U.S.C. Section 1734 solely to indicate this fact.

Received June 15, 2018; revised November 12, 2018; accepted April 24, 2019; published first May 1, 2019.

References

1. McGranahan N, Furness AJ, Rosenthal R, Ramskov S, Lyngaa R, Saini SK, et al. Clonal neoantigens elicit T cell immunoreactivity and sensitivity to immune checkpoint blockade. Science 2016;351:1463–9.
2. Lu YC, Yao X, Crystal JS, Li YF, El-Gamil M, Gross C, et al. Efficient identification of mutated cancer antigens recognized by T cells associated with durable tumor regressions. Clin Cancer Res 2014;20:3401–10.
3. Lauss M, Donia M, Harbst K, Andersen R, Mitra S, Rosengren F, et al. Mutational and putative neoantigen load predict clinical benefit of adoptive T cell therapy in melanoma. Nat Commun 2017;8:1738.
4. Schumacher TN, Schreiber RD. Neoantigens in cancer immunotherapy. Science 2015;348:69–74.
5. Le DT, Uram JN, Wang H, Bartlett BR, Kemberling H, Eyring AD, et al. PD-1 blockade in tumors with mismatch-repair deficiency. N Engl J Med 2015; 372:2509–20.
6. Rizvi NA, Hellmann MD, Snyder A, Kvistborg P, Makarov V, Havel JJ, et al. Cancer immunology. Mutational landscape determines sensitivity to PD-1 blockade in non-small cell lung cancer. Science 2015;348:124–8.
7. Anagnostou V, Smith KN, Forde PM, Niknafs N, Bhattacharya R, White J, et al. Evolution of neoantigen landscape during immune checkpoint blockade in non–small cell lung cancer. Cancer Discov 2017;7:264–76.
8. Forbes S, Beare D, Bindal N, Bamford S, Ward S, Cole C, et al. COSMIC: High-resolution cancer genetics using the catalogue of somatic mutations in cancer. Current Protoc Human Genet 2016;91:10.11.1-10.
9. Arcila ME, Chaft JE, Nafa K, Roy-Chowdhuri S, Lau C, Zaidinski M, et al. Prevalence, clinicopathologic associations, and molecular spectrum of ERBB2 (HER2) tyrosine kinase mutations in lung adenocarcinomas. Clin Cancer Res 2012;18:4910–8.
10. Pao W, Girard N. New driver mutations in non-small-cell lung cancer. Lancet Oncol 2011;12:175–80.
11. Marty R, Kaabinejadian S, Rossell D, Slifker MJ, van de Haar J, Engin HB, et al. MHC-I genotype restricts the oncogenic mutational landscape. Cell 2017;171:1272–83.
12. Marty R, Thompson WK, Salem RM, Zanetti M, Carter H. Evolutionary pressure against MHC class II binding cancer mutations. Cell 2018;175: 416–428.e13.
13. Philip M, Fairchild L, Sun L, Horste EL, Camara S, Shakiba M, et al. Chromatin states define tumour-specific T cell dysfunction and reprogramming. Nature 2017;545:452.
14. Spitzer MH, Carmi Y, Reticker-Flynn NE, Kwek SS, Madhireddy D, Martins MM, et al. Systemic immunity is required for effective cancer immunotherapy. Cell 2017;168:487–502.
15. Kreiter S, Vormehr M, van de Roemer N, Diken M, Löwer M, Diekmann J, et al. Mutant MHC class II epitopes drive therapeutic immune responses to cancer. Nature 2015;520:692–6.
16. Linnemann C, Van Buuren MM, Bies L, Verdegaal EM, Schotte R, Calis JJ, et al. High-throughput epitope discovery reveals frequent recognition of neo-antigens by CD4+ T cells in human melanoma. Nat Med 2015;21: 81.
17. Ott PA, Hu Z, Keskin DB, Shukla SA, Sun J, Bozym DJ, et al. An immunogenic personal neoantigen vaccine for patients with melanoma. Nature 2017;547:217.
18. Al-Shibli KI, Donnem T, Al-Saad S, Persson M, Bremnes RM, Busund LT. Prognostic effect of epithelial and stromal lymphocyte infiltration in non–small cell lung cancer. Clin Cancer Res 2008;14:5220–7.

19. Hiraoka K, Miyamoto M, Cho Y, Suzuoki M, Oshikiri T, Nakakubo Y, et al. Concurrent infiltration by CD8+ T cells and CD4+ T cells is a favourable prognostic factor in non-small-cell lung carcinoma. Br J Cancer 2006;94: 275.
20. Wakabayashi O, Yamazaki K, Oizumi S, Hommura F, Kinoshita I, Ogura S, et al. CD4+ T cells in cancer stroma, not CD8+ T cells in cancer cell nests, are associated with favorable prognosis in human nonsmall cell lung cancers. Cancer Sci 2003;94:1003–9.
21. Cibulskis K, Lawrence MS, Carter SL, Sivachenko A, Jaffe D, Sougnez C, et al. Sensitive detection of somatic point mutations in impure and heterogeneous cancer samples. Nat Biotechnol 2013;31:213.
22. Saunders CT, Wong WS, Swamy S, Becq J, Murray LJ, Cheetham RK. Strelka: accurate somatic small-variant calling from sequenced tumor–normal sample pairs. Bioinformatics 2012;28:1811–7.
23. McKenna A, Hanna M, Banks E, Sivachenko A, Cibulskis K, Kernytsky A, et al. The Genome Analysis Toolkit: a MapReduce framework for analyzing next-generation DNA sequencing data. Genome Res 2010; 20:1297–303.
24. Riddell SR, Greenberg PD. The use of anti-CD3 and anti-CD28 monoclonal antibodies to clone and expand human antigen-specific T cells. J Immunol Methods 1990;128:189–201.
25. Kargl J, Busch SE, Yang GH, Kim KH, Hanke ML, Metz HE, et al. Neutrophils dominate the immune cell composition in non-small cell lung cancer. Nat Commun 2017;8:14381.
26. Kreiter S, Selmi A, Diken M, Sebastian M, Osterloh P, Schild H, et al. Increased antigen presentation efficiency by coupling antigens to MHC class I trafficking signals. J Immunol 2008;180:309–18.
27. Veatch JR, Lee SM, Fitzgibbon M, Chow IT, Jesernig B, Schmitt T, et al. Tumor infiltrating BRAFV600E-specific CD4 T cells correlated with complete clinical response in melanoma. J Clin Invest 2018;128: 1563–8.
28. Tran E, Turcotte S, Gros A, Robbins PF, Lu YC, Dudley ME, et al. Cancer immunotherapy based on mutation-specific CD4+ T cells in a patient with epithelial cancer. Science 2014;344:641–5.
29. Jones S, Peng PD, Yang S, Hsu C, Cohen CJ, Zhao Y, et al. Lentiviral vector design for optimal T cell receptor gene expression in the transduction of peripheral blood lymphocytes and tumor-infiltrating lymphocytes. Hum Gene Ther 2009;20:630–40.
30. Lim CS, Brown CM. Hepatitis B virus nuclear export elements: RNA stem-loop α and β, key parts of the HBV post-transcriptional regulatory element. RNA Biol 2016;13:743–7.
31. Kuball J, Dossett ML, Wolfl M, Ho WY, Voss RH, Fowler C, et al. Facilitating matched pairing and expression of TCR chains introduced into human T cells. Blood 2007;109:2331–8.
32. Ren J, Liu X, Fang C, Jiang S, June CH, Zhao Y. Multiplex genome editing to generate universal CAR T cells resistant to PD1 inhibition. Clin Cancer Res 2016;23:2255–66.
33. Li H. Aligning sequence reads, clone sequences and assembly contigs with BWA-MEM. arXiv:13033997; 2013. Available from: https://arxiv.org/abs/1303.3997.
34. Li H, Durbin R. Fast and accurate short read alignment with Burrows–Wheeler transform. Bioinformatics 2009;25:1754–60.
35. McKenna A, Hanna M, Banks E, Sivachenko A, Cibulskis K, Kernytsky A, et al. The Genome Analysis Toolkit: a MapReduce framework for analyzing next-generation DNA sequencing data. Genome Res 2010;20:1297–303.
36. Van der Auwera GA, Carneiro MO, Hartl C, Poplin R, Del Angel G, LevyMoonshine A, et al. From FastQ data to high confidence variant calls: the genome analysis toolkit best practices pipeline. Curr Protoc Bioinformatics 2013;43:11.10.1-33.
37. Ramos AH, Lichtenstein L, Gupta M, Lawrence MS, Pugh TJ, Saksena G, et al. Oncotator: cancer variant annotation tool. Hum Mutat 2015;36: E2423–9.
38. Li B, Dewey CN. RSEM: accurate transcript quantification from RNA-Seq data with or without a reference genome. BMC Bioinformatics 2011;12:323.
39. Okamoto S, Mineno J, Ikeda H, Fujiwara H, Yasukawa M, Shiku H, et al. Improved expression and reactivity of transduced tumor-specific TCRs in human lymphocytes by specific silencing of endogenous TCR. Cancer Res 2009;69:9003–11.
40. Sahin U, Derhovanessian E, Miller M, Kloke BP, Simon P, Löwer M, et al. Personalized RNA mutanome vaccines mobilize poly-specific therapeutic immunity against cancer. Nature 2017;547:222.
41. Yossef R, Tran E, Deniger DC, Gros A, Pasetto A, Parkhurst MR, et al. Enhanced detection of neoantigen-reactive T cells targeting unique and shared oncogenes for personalized cancer immunotherapy. JCI Insight 2018;3. pii: 122467.
42. Zwaveling S, Mota SC, Nouta J, Johnson M, Lipford GB, Offringa R, et al. Established human papillomavirus type 16-expressing tumors are effectively eradicated following vaccination with long peptides. J Immunol 2002;169:350–8.
43. Karosiene E, Rasmussen M, Blicher T, Lund O, Buus S, Nielsen M. NetMHCIIpan-3. 0, a common pan-specific MHC class II prediction method including all three human MHC class II isotypes, HLA-DR, HLA-DP and HLA-DQ. Immunogenetics 2013;65:711–24.
44. Maiers M, Gragert L, Klitz W. High-resolution HLA alleles and haplotypes in the United States population. Hum Immunol 2007;68:779–88.
45. Cafri G, Yossef R, Pasetto A, Deniger DC, Lu YC, Parkhurst M, et al. Memory T cells targeting oncogenic mutations detected in peripheral blood of epithelial cancer patients. Nat Commun 2019;10:449.